RARE METALS

Interface structures and mechanical properties of corrugated + flat rolled and traditional rolled Mg/Al clad plates

Sha Li, Chao Luo, Muhammad-Umar Bashir, Yi Jia, Jian-Chao Han* , Tao Wang*

Abstract The corrugated + flat rolling (CFR) and traditional rolling (TR) methods were used to prepare Mg/Al clad plates using AZ31B Mg and 5052 Al plates, and the interface morphologies and mechanical properties of the resulting clad plates were compared. Examination of the microstructures of the plates showed that the TRed Mg/Al clad plate presented a straight interface, while a corrugated interface containing fractured intermetallic particulates was observed for the CFRed plate due to the inhomogeneous strain induced by the corrugated roller. During the CFR process, the corrugated roller can accelerate the rupture of the substrate work-hardening layers and facilitate the mutual extrusion of fresh metals to enhance the interface bonding. Compared with the traditional basal texture of the Mg alloy, the CFR process can change the texture morphology, thereby enhancing the plastic deformation ability of the Mg plate. Tensile tests showed that the CFRed Mg/Al clad plate exhibited a higher ultimate tensile strength (UTS, 316 MPa), which was ∼ 8% higher than that of the TRed plate (293 MPa). In addition, the bending curve of the CFRed clad plate was smooth and there was no stress sudden drop phenomenon in the bending process. The higher UTS and excellent bending properties of the CFRed clad plate could be attributed to the enhanced coordinated deformation ability of the substrates induced by the corrugated interface, grain refinement, and the change in the Mg alloy texture morphology.

Keywords Mg/Al clad plate; Corrugated + flat rolling; Traditional rolling; Interface morphologies; Mechanical properties

1 Introduction

Owing to their low density, good thermal conductivity, and high specific strength, Mg alloys have been employed widely in the automobile, aerospace, and electronic industries, and some other fields [1–3]. However, their poor oxidation and corrosion resistances limit their further application [4–6]. In contrast, Al alloys exhibiting good plasticity are environmentally friendly light engineering materials, and they can form compact oxide films to prevent corrosion [7–9]. Al alloys can therefore be formed and processed using a range of methods, and so have been widely employed in shipbuilding, marine engineering, and in oil and gas storage [10–12]. Thus, Mg/Al clad plates exhibit a combination of these properties, being lightweight and low cost, in addition to having high specific strength, and good corrosion resistance [13–15]. Such materials are therefore expected to be applicable in the aviation, aerospace, nautical, and national defense industries [16–18].

A number of methods currently exist for the fabrication of Mg/Al clad plates, including explosive welding, explosive welding + rolling, diffusion, and hot rolling. For example, Zhang et al. [19] successfully prepared Mg/Al

S. Li, C. Luo, M.-U. Bashir, Y. Jia, J.-C. Han*, T. Wang*
College of Mechanical and Vehicle Engineering, Taiyuan
University of Technology, Taiyuan 030024, China
e-mail: hanjianchao@tyut.edu.cn

T. Wang
e-mail: tyutwt@163.com

S. Li, C. Luo, M.-U. Bashir, Y. Jia, J.-C. Han, T. Wang
Engineering Research Center of Advanced Metal Composites
Forming Technology and Equipment, Ministry of Education,
Taiyuan 030024, China

S. Li, C. Luo, M.-U. Bashir, Y. Jia, J.-C. Han, T. Wang
TYUT-UOW Joint Research Center, Taiyuan University of
Technology, Taiyuan 030024, China

clad plates using the explosive welding method. The interface of their plate presented a small wave shape, and an adiabatic shear band existed on the Mg-side close to the interface. In addition, Chen et al. [20] reported that the tensile strength of Mg/Al clad plates manufactured by explosive welding + 5 passes of hot rolling initially increased prior to decreasing upon increasing the annealing temperature and holding time. However, the explosive process results in significant environmental pollution and a number of safety hazards. Liu et al. [21] obtained Mg/Al clad plates via a vacuum diffusion technique; however, the required equipment was complex and expensive, and this method is not conducive for large-scale production due to the long production cycle. As another example, Nie et al. [22] produced three-layered Al/Mg/Al plates at 400 °C and subsequent annealing at 200–400 °C for 1–4 h. They found that thick intermetallics formed at the interface of the plates annealed at 400 °C, which greatly weakened the bonding strength. Among these methods, the hot rolling method is increasing in popularity due to its simplicity, low cost, and facile continuous production.

Recently, a new rolling process, namely corrugated + flat rolling (CFR), was proposed for the production of Cu/Al clad plates under the 20% reduction ratio, and remarkable improvements in the plate tensile properties were observed [23]. Furthermore, this method was also reported for the fabrication of Mg/Al clad plates, resulting in an enhancement in the ultimate tensile strength (UTS) [24, 25]. However, the differences between the Mg/Al clad plates manufactured by the CFR method and the traditional rolling (TR) method have yet to be examined. Thus, we herein report the preparation of Mg/Al clad plates with the same final thickness using the two rolling methods. Microstructural observations of the interface are carried out in addition to the determination of the plate mechanical properties using scanning electron microscopy (SEM), X-ray diffraction (XRD) measurements, electron backscatter diffraction (EBSD) analysis, tensile experiments, and three-point bending tests. The microstructural evolutions and mechanical behaviors are then discussed in detail.

2 Experimental

An AZ31B Mg plate and a 5052 Al plate were chosen as the substrates. Dimensions of these matrix materials were 100 mm × 60 mm × 2 mm. Prior to the rolling experiment, the bonding surfaces of the Mg and Al plates were polished using a steel wire brush to remove any oxides or oil stains. The Mg and Al plates were then assembled and bound to make a blank. Finally, the prepared blank was placed into a vacuum heating furnace at 400 °C under an argon atmosphere for 15 min. For the TR method, after heat treatment, the Mg/Al blank was directly placed into the rolling mill where the upper and lower rollers were conventional flat rollers, and the reduction ratio was 51.25%. For the CFR method, two rolling passes were employed. More specifically, the first pass involved corrugated rolling at 35% reduction ratio, where the Mg plate was in contact with the upper corrugated roller and the Al plate was in contact with the lower flat roller. A corrugated Mg/Al clad plate with a wavy Mg surface was obtained after the first corrugated pass. The second pass involved flat rolling at 25% reduction ratio, and this gave the finished plate with a flat Mg surface. Intermediate heat treatment at 400 °C was conducted for 5 min between these two passes. The Mg/Al clad plates were produced using a two-high laboratory mill (150 mm diameter) without lubricant. The surface of the corrugated roller was a sinusoidal curve with an amplitude of 0.5 mm and a period of 0.06 rad. Flat Mg/Al clad plates with equal final thickness (i.e., 1.95 mm) were obtained using these two rolling processes. Figure 1 shows a schematic representation of the CFR and TR methods for preparation of the Mg/Al clad plates.

The metallographic samples of the prepared Mg/Al clad plate were cut using a wire cutting machine, and the surface of the rolling direction and the normal direction (RD-ND) plane was sanded with 600, 1000, 2000, and 4000 mesh sandpapers. The surfaces to be analyzed were polished with an alumina solution until the surfaces presented a mirror effect. The interface characteristics of the samples were observed using SEM (JEOL-IT500) combined with energy-dispersive spectroscopy (EDS) and EBSD. XRD (Bruker D8) was used to identify the interface phase composition. A 5969 universal tensile testing machine was employed to test the tensile strength, and for this purpose, a tensile rate of 0.5 mm·min^{-1} and a three-point bending strength with a bending rate of 3 mm·min^{-1} were used. Tensile samples were cut from the Mg/Al clad plate along the transverse direction (TD). The gauge length and width of tensile specimens were 20 and 5 mm, respectively. The length and width of the three-point bending samples were 45 and 5 mm, respectively.

3 Results

3.1 Interface microstructure

Figure 2 shows the interface SEM image of the CFRed Mg/Al clad plate, where the bonding interface presents an obvious corrugated shape structure. During the first corrugated pass, a sample with a severe corrugated surface structure for the upper Mg plate was produced due to the local strong stress induced by the corrugated roller. In
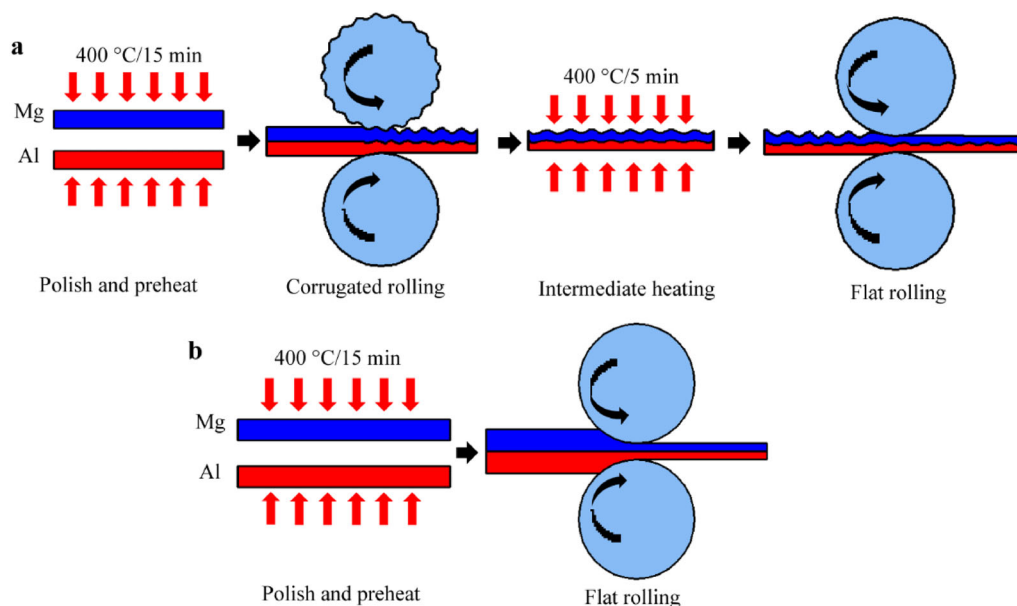
Fig. 1 Schematic representation of rolling methods employed herein: **a** CFR, **b** TR
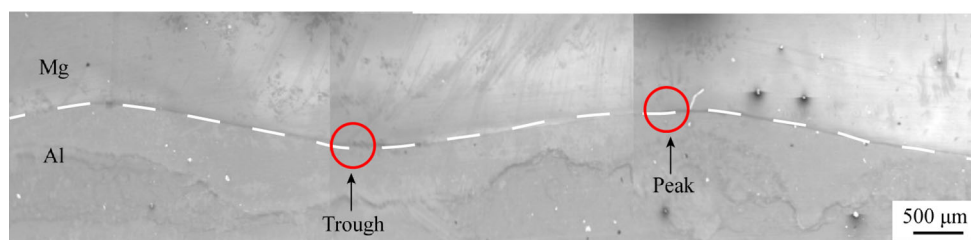

Fig. 2 Interface SEM image of CFRed Mg/Al clad plate

contrast, during the second flat pass, the Mg material protruding after the first pass extended downward and on both sides under the action of rolling force, forming a trough position. The stress imparted on the concave Mg metal surface during the second pass was relatively small, and so a peak was formed, as shown in Fig. 2. Due to the nonuniform strain at different interface positions, corrugated interface was obtained for the CFRed clad plate. To facilitate the subsequent analysis, the "peak" and "trough" (as marked in Fig. 2) can be used to represent the typical interface positions according to the corrugated shape.

Figure 3 shows the interface SEM images, elemental distribution diagrams, and corresponding EDS line scanning results for the Mg/Al clad plates prepared using these two different rolling processes. More specifically, Fig. 3a shows the TRed interface, while Fig. 3b, c displays the CFRed interface at the peak position and trough position, respectively. As can be seen from Fig. 3a, the TRed Mg/Al interface was tightly bonded without holes and cracks under the large reduction ratio of 51.25%. According to the Line 1 scan result (Fig. 3a), sharp drops in the Mg and Al contents were observed at the bond interface, indicating

that no intermetallic compounds (IMCs) were formed at the interface [26]. The interface morphologies of the CFRed clad plate (Fig. 3b, c) were found to differ significantly from that of the TRed clad plate (Fig. 3a). The interface of the CFRed clad plate was not continuously distributed, but instead, presented a fractured zigzag shape both at the peak and the trough positions. It can be seen from the elemental distribution diagrams in Fig. 3b, c that the interface zigzag regions contained significant quantities of Mg and Al. The platform can be observed at the Mg/Al interface, as indicated in EDS Line 2 (Fig. 3b), which indicates that stable IMCs formed at the zigzag regions with a thickness of ~ 13 μm. These hard and brittle IMCs were generated during the intermediate heat treatment between the first corrugated pass and the second flat pass.

As described in the literature [27], the IMCs are composed of two layers, namely $Mg_{17}Al_{12}$ close to the Mg-side, and Mg_2Al_3 close to the Al-side. During the second flat pass, the IMCs were found to break with the prolongation of the Mg/Al plate. From the peak (Fig. 3b) and trough positions (Fig. 3c), a newly formed interface can be observed between the fractured IMCs at the interface of the
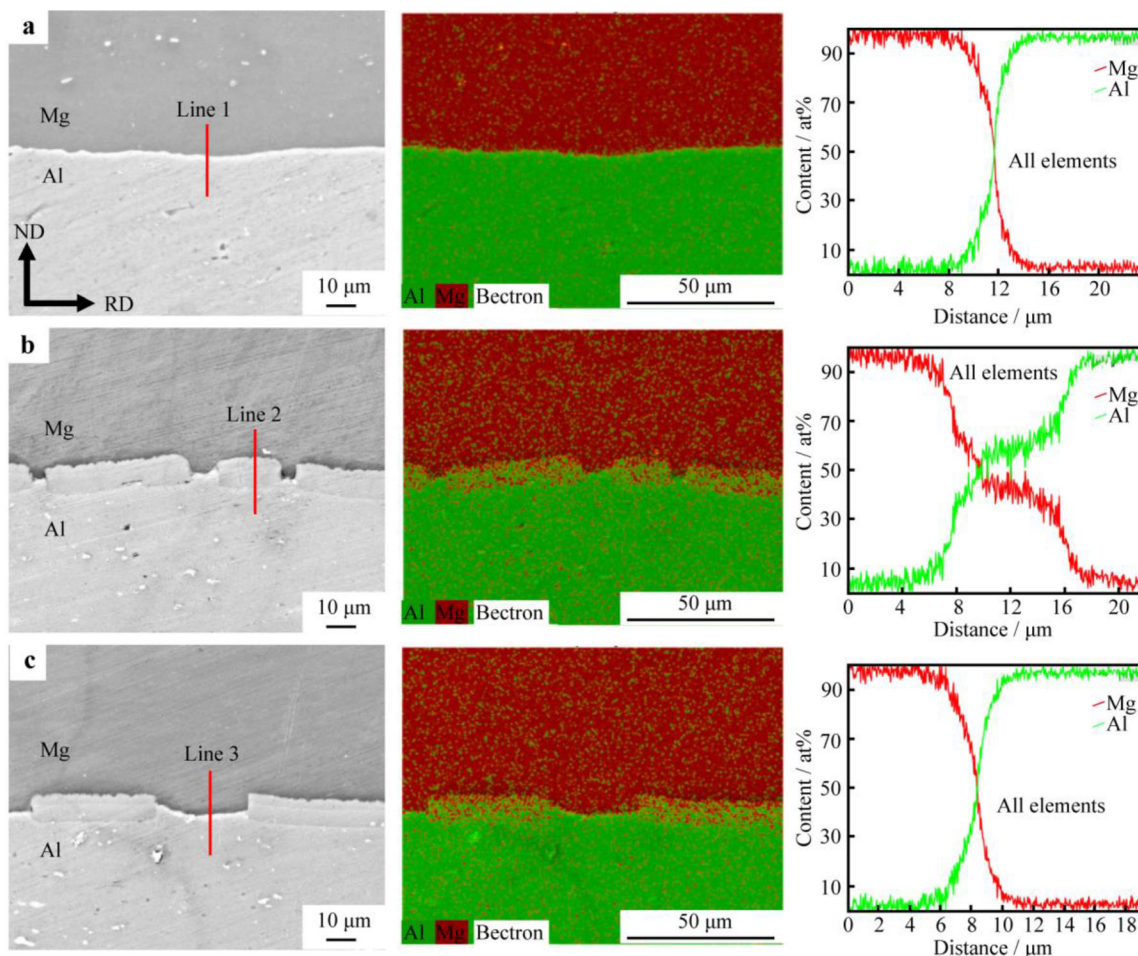
Fig. 3 SEM images of Mg/Al interfaces: **a** TR, **b** CFR peak, **c** CFR trough

CFRed clad plate. However, no cracks, holes, or stable IMCs were observed at the new interface according to EDS Line 3 shown in Fig. 3c.

To further determine the phase compositions at the interface of the CFRed and TRed clad plates, XRD was carried out on the bonding surface both at the Mg- and Al-sides. As indicated in Fig. 4a, b, for the TRed specimen, no additional phase was observed except for the base Mg and Al phases at the interface. In contrast, for the CFRed specimen, $Mg_{17}Al_{12}$ and Mg_2Al_3 phases could be detected on the Mg-side (Fig. 4c), while Mg_2Al_3 was detected on the Al-side (Fig. 4d). This confirmed the existence of IMCs at the interface of the CFRed clad plate and indicated that these hard and brittle IMCs formed at the CFRed specimen interface during the intermediate annealing treatment. Moreover, fractures formed within the Mg_2Al_3 layer because of the brittleness for the Mg_2Al_3 [27].

3.2 Crystal structure

To investigate the influences of these two rolling processes on the crystal structure of matrix Mg and matrix

Al, interface EBSD analysis was carried out. As shown in Fig. 5a, after the TR deformation process, the mixed grains of finer and coarse equiaxed grains formed by dynamic recrystallization (DRX) were distributed at the Mg-side, while the Al grains were elongated along the RD with a large number of fine grains at the grain boundary. It was worth noting that fine equiaxed grains also appeared at the Mg-side after the CFR process for both the peak (Fig. 5b) and the trough positions (Fig. 5c) [28]. Compared with the TRed clad plate (Fig. 5a), it should be noted that the grains close to the Mg/Al interface were smaller than those further from the interface of the CFRed clad plate; this phenomenon was more pronounced at the trough position (Fig. 5c). The average Mg grain size was 2.83 μm at the peak of the CFRed clad plate, and 2.55 μm at the trough, indicating finer grains than those of the TRed clad plate (3.53 μm). In addition, many Al grains at the peak position (Fig. 5b) still maintained the coarse equiaxed state, but the Al grains were elongated along the RD at the trough position (Fig. 5c), and many finer sub-grains formed at the Al grain boundary.
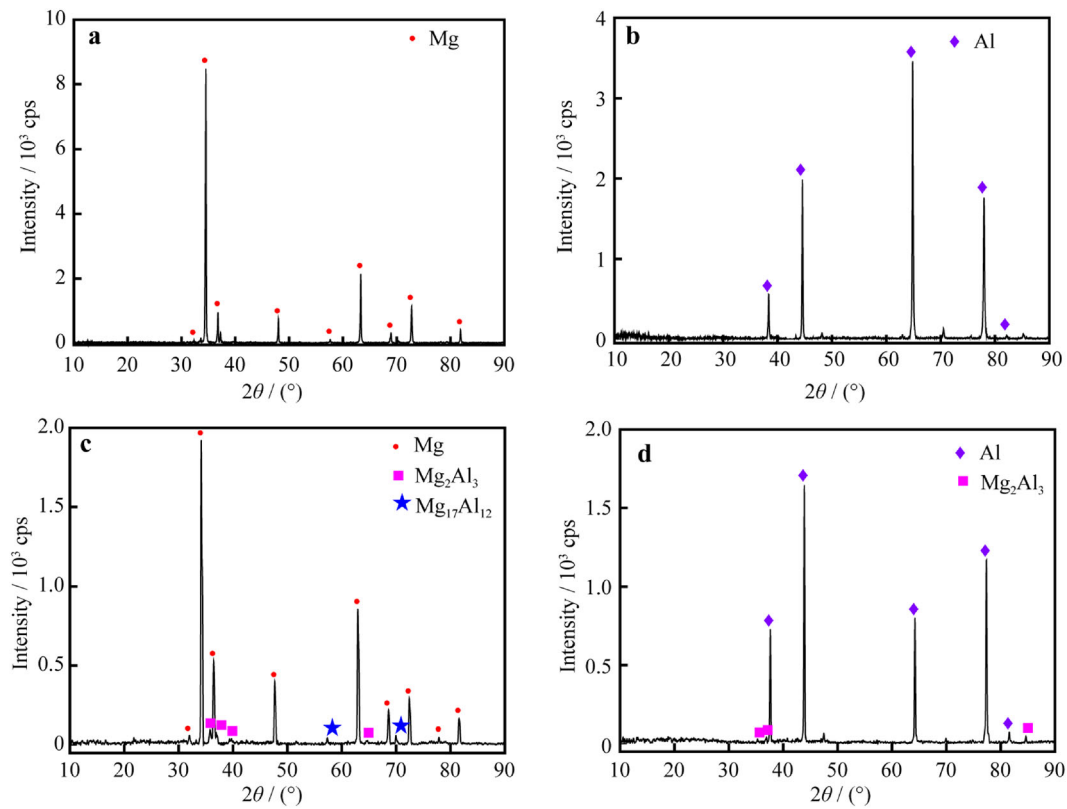
Fig. 4 XRD patterns of bonding surfaces: **a** Mg-side of TR, **b** Al-side of TR, **c** Mg-side of CFR, **d** Al-side of CFR
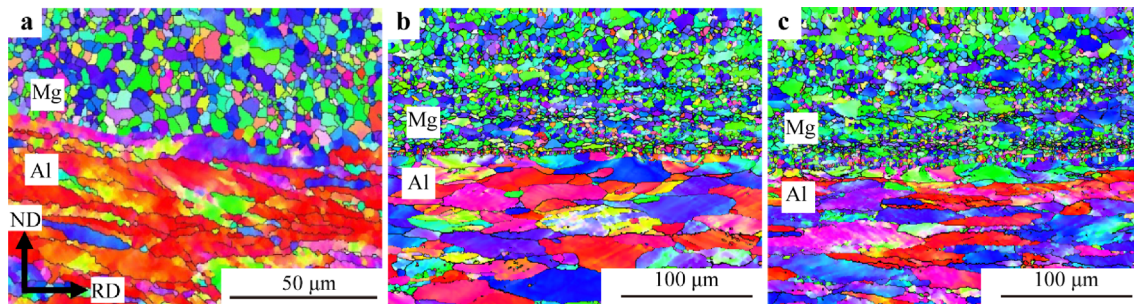

Fig. 5 Inverse pole figure (IPF) maps of bonding interfaces: **a** TR, **b** CFR peak, **c** CFR trough

3.3 Texture and misorientation angle

Figure 6 shows the (0001) pole figure (PF) of the Mg alloy and the (111) pole figure of the Al alloy, as well as the misorientation angle distribution of the substrate metals after these two rolling processes. It can be seen from Fig. 6a that the c-axis of the TRed Mg grains was parallel to the ND, which was the typical basal texture. Following the CFR process, the c-axis of the Mg grains at the trough position (Fig. 6c) was parallel to the ND, giving a basal texture, while the c-axis of the Mg grains at the peak position (Fig. 6b) rotated 90° parallel to the TD. Greater stress was therefore required to satisfy the larger critical resolved shear stress (CRSS) when deactivating the <

c+a> slip. Since the CRSS of the basal <a> slip is ∼ 0.45–0.81 MPa, the prismatic <a> slip is ∼ 39.2 MPa, and the pyramidal <c+a> slip is ∼ 45–81 MPa [29]. Therefore, the CFR process can result in rotation of the c-axis of the Mg grains, which can improve the plastic deformation ability of the Mg plate and enhance the yield strength of the Mg/Al clad plate. In terms of the Al plate, no obvious macroscopic texture was formed at the Al-side in the TR (Fig. 6d) or the CFR process (Fig. 6e, f). As a result, Al plate will exhibit good plastic deformation behavior in the plastic deformation process.

During the TR process, high angle grain boundaries (HAGBs) (> 15°) of the Mg alloy accounted for a large proportion (i.e., 71.1%), while the content of low angle
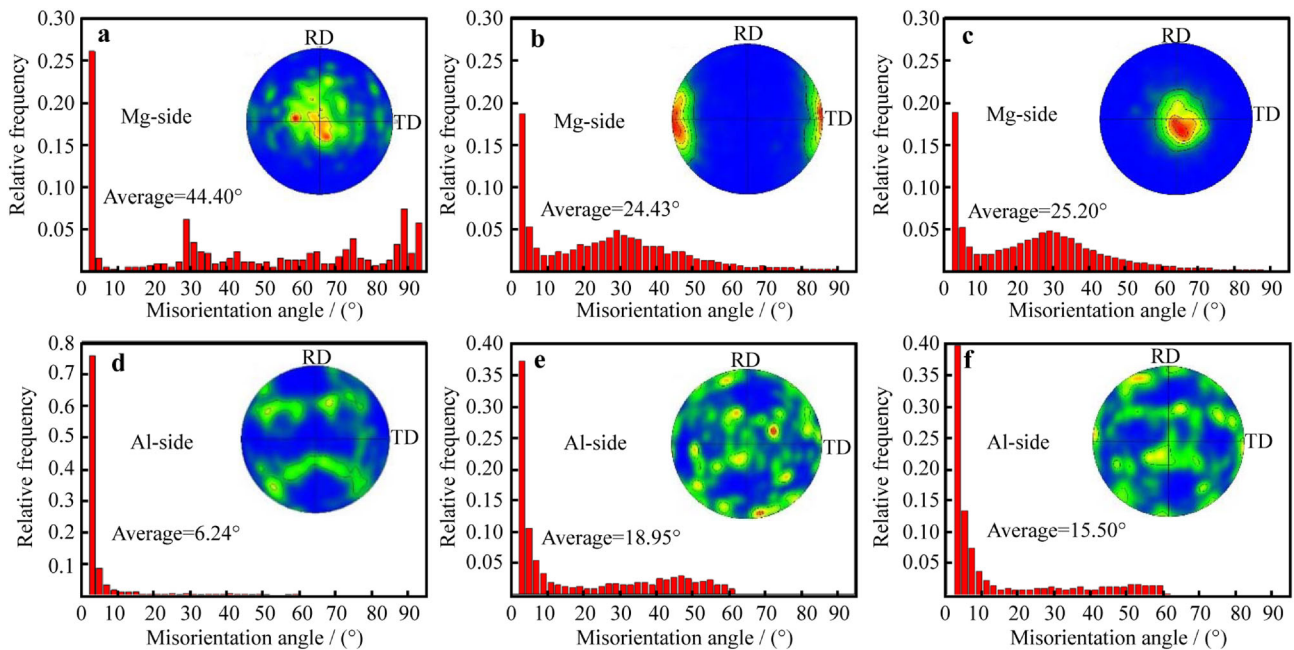
Fig. 6 PF maps and misorientation angle of substrates: **a**, **d** TR; **b**, **e** CFR peak; **c**, **f** CFR trough

grain boundaries (LAGBs) (2–15°) was only of 28.9%, thereby giving an average misorientation angle of 44.4° (Fig. 6a). In addition, significant peak values were observed at ∼ 30° and 86° (Fig. 6a), which indicated that dynamic recrystallization took place, and tensile twins formed at the Mg-side of the TRed clad plate [30]. The percentage of LAGBs for the Mg was 57.00% at the peak position (Fig. 6b) and 54.18% at the trough position (Fig. 6c), while that of HAGBs was 43.00% (Fig. 6b) and 45.82% (Fig. 6c), respectively, for the CFRed clad plate. Compared with that in the TR process, the proportion of LAGBs at the Mg-side increased after the CFR process. Thus, the average misorientation angle of the Mg alloy decreased to 24.43° at the peak position (Fig. 6b) and 25.2° at the trough position (Fig. 6c). Moreover, a clear peak value formed at 30° for both peak and trough positions, which indicated that dynamic recrystallization occurred at the Mg-side.

In terms of the Al alloy plate, LAGBs accounted for a large proportion (i.e., 92.2%) of the TRed clad plate, giving an average misorientation angle of 6.24° (Fig. 6d), thereby indicating a high dislocation density. Meanwhile, the proportions of LAGBs at the peak position (Fig. 6e) and the trough position (Fig. 6f) of the CFRed clad plate decreased, giving values of 67.63% and 76.75%, respectively. The average misorientation angle increased to 18.95° at the peak (Fig. 6e) and 15.50° at the trough (Fig. 6f), which indicated that the dislocation density decreased compared with that obtained using the TR process.

3.4 Tensile test

Figure 7a shows the tensile curves of the Mg/Al clad plates along the TD at room temperature, where it can be seen that the UTS of the CFRed clad plate was 316 MPa, which was ∼ 8% higher than that of the TRed clad plate (293 MPa). However, the fracture elongation of the CFRed clad plate was 13%, which was lower than that of the TRed clad plate (15%). Although the UTS of the CFRed clad plate likely increased due to fine grain strengthening, the work-hardening phenomenon resulting from two passes of the CFR process resulted in a decrease in the fracture elongation.

Although there were differences in the UTS and fracture elongation of the Mg/Al clad plates prepared using the two different rolling methods, it can be seen from the tensile curves (Fig. 7a) that the stress suddenly dropped and then rebounded slightly in both cases. During the tensile process, the Mg plate broke initially due to its brittle nature, while with further development of the tensile process, delamination occurred along the Mg/Al interface. Ultimately, the Al plate exhibiting superior plasticity continued to extend until fracture. This accounted for the sudden decrease and subsequent increase in the tensile stress, which was ultimately due to interface delamination. In addition, Fig. 7b shows the macro-tensile fracture diagrams of the Mg/Al clad plates, where it can be seen that two substrates of the TRed clad plate had undergone complete stratification at the gauge position after the tensile process. In contrast, the CFRed clad plate was still in combination,
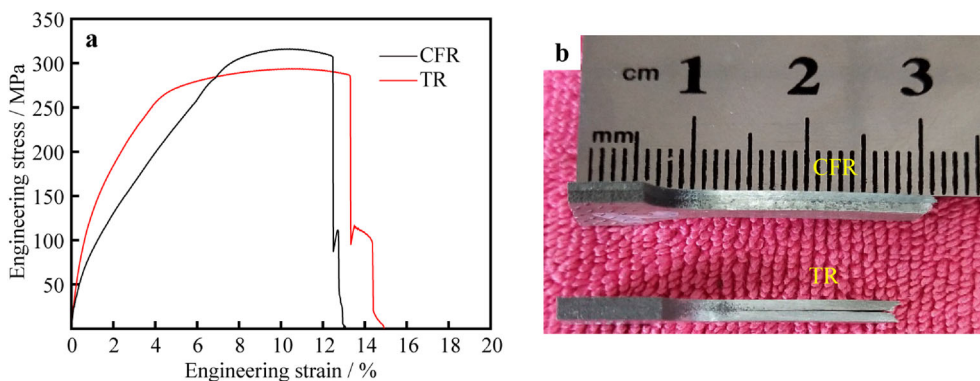
Fig. 7 **a** Tensile curves of Mg/Al clad plates, **b** macro-tensile fracture diagrams

which could be mainly attributed to its corrugated interface.

3.5 Bending test

Figure 8 shows the three-point bending curves of the clad plates along the RD at room temperature, where it can be seen that the bending strength of the CFRed clad plate was 400 MPa, while that of the TRed clad plate was higher (415 MPa). However, the yield strength of the former was 345 MPa, which was a higher value than that recorded for the latter (280 MPa). It can also be seen from the bending curve of the TRed clad plate that the load dropped abruptly when the strain was 14%, and this was mainly caused by interface delamination and Mg sheet creaking. While this was not observed for the CFRed clad plate, the load dropped smoothly after exceeding the maximum stress value. Figure 9 displays the interface bending fracture SEM images of the Mg/Al clad plates after the bending tests. It can be seen that fractures were observed on the Mg-side and on the interface, and the extruded Mg metal blocks can be observed for the TRed clad plate (Fig. 9a). However, no cracks were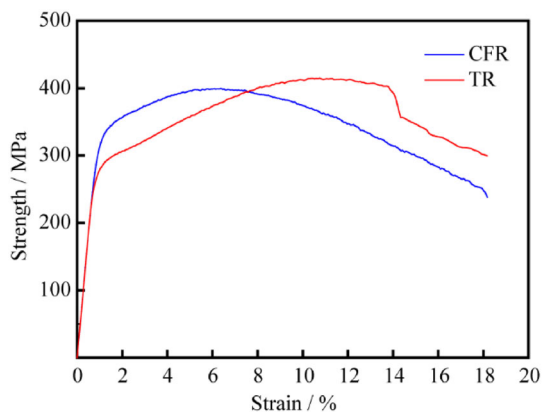 observed on the substrates after the bending tests, and no delamination took place at the interface of the CFRed clad plate (Fig. 9b).

4 Discussion

4.1 Interface bonding behavior

The stress state acting on the Mg/Al clad plates prepared by the CFR and TR methods differs. During the CFR deformation process, the corrugated roller imposes an inhomogeneous strain distribution between Mg matrix and Al matrix, which can lead to a high strain at the trough position and a low strain at the peak position. In contrast, the stress induced by the traditional flat roller on the Mg/Al clad plate appears to be homogeneous. While friction deformation is dominant in the TR process, shear deformation behavior caused by the inhomogeneous stress is also observed in the CFR process [31]. The obvious shear stress induced by the corrugated roller can cause tearing of the metal surface, which results in fresh metal being squeezed into the opposite matrix to form a bond, which further enhances the interface bonding [32, 33]. Moreover, the corrugated interface can increase the contact areas between the Mg plate and the Al plate and promote the interface combination of the CFRed clad plate, which differs significantly from the flat interface of the TRed clad plate.

As shown in Fig. 5b, c, finer Mg grains can be observed in the CFRed Mg/Al clad plate. The formation of these fine Mg grains can be attributed to the DRX phenomenon, where new grains nucleate and grow in the deformed grains when the metals deform at a certain temperature [34]. A high strain can enhance the nucleation rate of recrystallization, which promotes the formation of finer grains [3]. In addition, the DRX temperature drops with an increase in the deformation strain, which also promotes DRX in these grains. Furthermore, the Mg plate exhibiting hexagonal close-packed structure and low stacking fault energy is
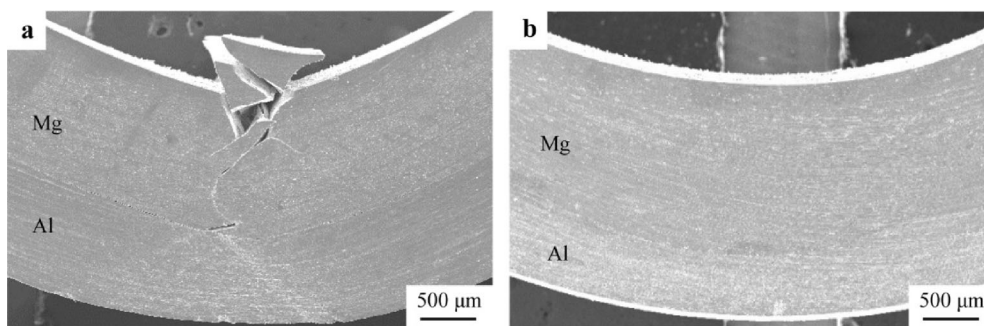

Fig. 8 Three-point bending stress–strain curves of Mg/Al clad plate

Fig. 9 SEM side view images of clad plates after bending tests: **a** TR, **b** CFR

prone to DRX when the temperature and strain are relatively low. Corrugated rolling can therefore produce a high strain at the Mg/Al interface, which can refine the Mg grains and improve the interface bonding strength.

4.2 Mechanical behavior

During the intermediate heat treatment process, continuous IMCs layer is generated, which greatly weakens the mechanical properties of the clad plates [24]. During the second flat pass, swelling Mg metals flow forward under the action of the rolling force, and the clad plate is extended along the RD [35]. As a result, elongation of the CFRed clad plate, especially the AZ31B Mg plate, is significantly improved, which is fully compatible with the plastic deformation between the AZ31B Mg and the 5052 Al sheets. In addition, the shear strain at the bonding interface caused by the CFR process changes the stress state between Mg and Al, thereby promoting larger shear deformation zones at both the peak and the trough of the CFRed clad plate. Furthermore, as shown in Fig. 5, the average Mg grain size of the CFRed clad plate is smaller than that of the TRed Mg grains, which can contribute to a higher strength due to fine grain strengthening. Moreover, the hard and brittle IMCs formed during intermediate heating break due to the formation of corrugated interface and newly formed interface, which can improve the interface combination and mechanical behavior of the CFRed clad plate [25]. When the CFRed Mg/Al clad plate is subjected to tensile stress or bending stress, the IMCs exhibiting fracture distribution at the interface can hinder delamination of the interface.

In contrast to the Mg alloy basal texture of the TRed clad plate, the CFR method induces a special texture configuration in the Mg alloy. It should be noted here that the basal texture of the TRed Mg alloy will affect the plastic formability of the plate. Moreover, a change in the texture morphology at the peak and trough of the CFRed Mg alloy can greatly enhance elongation of the Mg plate and increase the collaborative deformation ability between the Mg and Al plates, thereby improving the interface bonding of the CFRed clad plate. Compared to the TRed clad plate, it is apparent that alternation of the Mg alloy texture and the corrugated interface is conducive to improving the bending resistance of the Mg alloy of the CFRed clad plate.

5 Conclusion

Corrugated + flat rolling (CFR) and traditional rolling (TR) methods were applied for the preparation of Mg/Al clad plates, and subsequent comparison of the interface morphologies and mechanical properties of the resulting clad plates were reported. It was found that a flat interface was presented in the TRed Mg/Al clad plate, whereas a corrugated interface was observed in the CFRed clad plate, likely due to the inhomogeneous strain induced by the corrugated roller. In addition, in contrast to the Mg alloy basal texture of the TRed clad plate, the Mg alloy texture of the CFRed clad plate was found to vary with different interface positions. The finer Mg alloy grains of the CFRed clad plate were attributed to the dynamic recrystallization induced by the local high stress. Finally, the greater ultimate tensile strength and excellent bending properties of the CFRed Mg/Al clad plate were considered to result from the enhanced coordinated deformation between the Mg plate and the Al plate, which in turn was caused by the corrugated interface structure, grain refinement, and the changes in the Mg alloy texture.

References

[1] Yang XW, Feng WY, Li WY, Dong XR, Xu YX, Chu Q, Yao ST. Microstructure and properties of probeless friction stir spot welding of AZ31 magnesium alloy joints. Trans Nonferrous Met Soc. 2019;29(11):2300.

[2] Liu JB, Zhang K, Han JT, Li XG, Li YJ, Ma ML, Yuan JW, Shi GL. Microstructure and texture evolution of Mg–7Y–1Nd–0.5Zr alloy sheets with different rolling temperatures. Rare Met. 2020; 39(11):1273.

[3] Tang JW, Chen L, Zhao GQ, Zhang CS, Yu JQ. Study on Al/Mg/Al sheet fabricated by combination of porthole die co-extrusion and subsequent hot rolling. J Alloy Compd. 2019;784: 727.

[4] Li MF, Zhu ZQ, Zhang YF, Pan D, Xiao QK. AZ31Mg/6061Al ultrasonic welding and interface performance analysis. Chin J Rare Met. 2019;43(6):577.

[5] Ding HL, Zhang P, Cheng GP, Kamado S. Effect of calcium addition on microstructure and texture modification of Mg rolled sheets. Trans Nonferrous Met Soc. 2015;25(9):2875.

[6] Li XB, Yang Y, Xu YS, Zu GY. Deformation behavior and crack propagation on interface of Al/Cu laminated composites in uniaxial tensile test. Rare Met. 2018;39(3):296.

[7] Naseri M, Reihanian M, Borhani E. Bonding behavior during cold roll-cladding of tri-layered Al/brass/Al composite. J Manuf Process. 2016;24:125.

[8] Hoseini Athar MM, Tolaminejad B. Weldability window and the effect of interface morphology on the properties of Al/Cu/Al laminated composites fabricated by explosive welding. Mater Des. 2015;86:516.

[9] Jiang J, Liu Y, Xiao G, Wang Y, Ju Y. Effect of pass reduction on microstructure, mechanical properties and texture of hot-rolled 7075 alloy. Mater Charact. 2019;147:324.

[10] Quadir MZ, Najafzadeh N, Munroe PR. Variations in through-thickness recrystallization and grain growth textures in the Al layers in ARB-processed Al/Al(0.3% Sc) composite sheets. Mater Des. 2016;93:467.

[11] Li XB, Zu GY, Wang P. Asymmetry in interface and bending property of Al/Cu/Al bimetallic laminates. Rare Met. 2014; 33(5):556.

[12] Li Y, Wang QP, Gao GJ, Li JD, Wang ZD, Xu GM. Texture evolution and mechanical properties of Al–Mg–Si alloys at different intermediate annealing temperatures. Rare Met. 2019; 38(10):937.

[13] Li G, Yang W, Jiang W, Guan F, Jiang H, Wu Y, Fan Z. The role of vacuum degree in the bonding of Al/Mg bimetal prepared by a compound casting process. J Mater Process Technol. 2019; 265:112.

[14] Habila W, Azzeddine H, Mehdi B, Tirsatine K, Baudin T, Helbert AL, Brisset F, Gautrot S, Mathon MH, Bradai D. Investigation of microstructure and texture evolution of a Mg/Al laminated composite elaborated by accumulative roll bonding. Mater Charact. 2019;147:242.

[15] Wu Y, Xin YC, Xia XS, Feng B, Wang YB, Zhao ZD. Influence of annealing treatments on microstructure and mechanical properties of an extruded Mg AZ31/Al 7050 laminate. Acta Metall Sin Engl. 2018;32(2):227.

[16] Zhu C, Sun L, Gao W, Li G, Cui J. The effect of temperature on microstructure and mechanical properties of Al/Mg lap joints manufactured by magnetic pulse welding. J Mater Res Technol. 2019;8(3):3270.

[17] Zeng XY, Wang YX, Li XQ, Li XJ, Zhao TJ. Effect of inert gas-shielding on the interface and mechanical properties of Mg/Al explosive welding composite plate. J Manuf Process. 2019; 45:166.

[18] Wei AL, Liu XH, Dong L, Liang W. Binding property of Al/Mg/Al thin plates fabricated by one-pass hot rolling with different reduction ratios, temperatures and annealing treatments. Rare Met. 2015;37(2):136.

[19] Zhang TT, Wang WX, Zhang W, Wei Y, Cao XQ, Yan ZF, Zhou J. Microstructure evolution and mechanical properties of an AA6061/AZ31B alloy plate fabricated by explosive welding. J Alloy Compd. 2018;735:1759.

[20] Chen ZQ, Wang DY, Cao XQ, Yang WW, Wang WX. Influence of multi-pass rolling and subsequent annealing on the interface microstructure and mechanical properties of the explosive welding Mg/Al composite plates. Mater Sci Eng A. 2018;723: 97.

[21] Liu WS, Long LP, Ma YZ, Wu L. Microstructure evolution and mechanical properties of Mg/Al diffusion bonded joints. J Alloy Compd. 2015;643:34.

[22] Nie HH, Liang W, Chen HS, Zheng LW, Chi CZ, Li XR. Effect of annealing on the microstructures and mechanical properties of Al/Mg/Al laminates. Mater Sci Eng A. 2018;732:6.

[23] Wang T, Li S, Ren ZK, Han JC, Huang QX. A novel approach for preparing Cu/Al laminated composite based on corrugated roll. Mater Lett. 2019;234(1):79.

[24] Wang T, Li S, Ren ZK, Jia Y, Fu WS, Guo M, Ma XC, Han JC. Microstructure characterization and mechanical property of Mg/Al laminated composite prepared by the novel approach: corrugated + flat rolling (CFR). Metals. 2019;9(6):690.

[25] Wang T, Wang YL, Bian LP, Huang QX. Microstructural evolution and mechanical behavior of Mg/Al laminated composite sheet by novel corrugated rolling and flat rolling. Mater Sci Eng A. 2019;765:138318.

[26] Zhang N, Wang WX, Cao XQ, Wu JQ. The effect of annealing on the interface microstructure and mechanical characteristics of AZ31B/AA6061 composite plates fabricated by explosive welding. Mater Des. 2015;65:1100.

[27] Nie HH, Liang W, Zheng LW, Ren XX, Chi CZ. The microstructure, texture and mechanical properties of the rolled Al/Mg/Al clad sheets. J Mater Eng Perform. 2016;25(11):4695.

[28] Nie HH, Hao XW, Chen HS, Kang XP, Wang TL, Mi YJ, Liang W. Effect of twins and dynamic recrystallization on the microstructures and mechanical properties of Ti/Al/Mg laminates. Mater Des. 2019;181:107948.

[29] Wan G, Wu BL, Zhang YD, Sha GY, Esling C. Anisotropy of dynamic behavior of extruded AZ31 magnesium alloy. Mater Sci Eng A. 2010;527(12):2915.

[30] Tan JC, Tan MJ. Dynamic continuous recrystallization characteristics in two stage deformation of Mg–3Al–1Zn alloy sheet. Mater Sci Eng A. 2003;339(1):124.

[31] Li XB, Zu GY, Wang P. Effect of strain rate on tensile performance of Al/Cu/Al laminated composites produced by asymmetrical roll bonding. Mater Sci Eng A. 2013;575:61.

[32] Yousefi Mehr V, Toroghinejad MR, Rezaeian A. Mechanical properties and microstructure evolutions of multilayered Al–Cu composites produced by accumulative roll bonding process and subsequent annealing. Mater Sci Eng A. 2014;601:40.

[33] Hosseini SA, Hosseini M, Danesh Manesh H. Bond strength evaluation of roll bonded bi-layer copper alloy strips in different rolling conditions. Mater Des. 2011;32(1):76.

[34] Chu Q, Zhang M, Li J, Yan C. Experimental and numerical investigation of microstructure and mechanical behavior of titanium/steel interfaces prepared by explosive welding. Mater Sci Eng A. 2017;689:323.

[35] Kudo S, Yokoyama S, Shimoyama K, Kaneko S, Fujita F. Effect of dimple patterning conditions of periodical straining rolling on microstructures and mechanical properties of AZ31 sheets. Mater Sci Eng A. 2017;680:75.